

Workflow and intervention times of MR-guided focused ultrasound – Predicting the impact of new techniques



Arjo J. Loeve^{a,*}, Jumana Al-Issawi^b, Fabiola Fernandez-Gutiérrez^c, Thomas Langø^d, Jan Strehlow^b, Sabrina Haase^b, Matthias Matzko^e, Alessandro Napoli^f, Andreas Melzer^c, Jenny Dankelman^a

^a Delft University of Technology, Faculty of Mechanical, Maritime and Materials Engineering, Department of BioMechanical Engineering, TUD-3mE-BmechE, Mekelweg 2, 2628 CD Delft, The Netherlands

^b Fraunhofer MEVIS, Institute for Medical Image Computing, Universitätsallee 29, 28359 Bremen, Germany

^c University of Dundee, College of Medicine, Institute for Medical Science and Technology, Division of Imaging and Technology, Wurzburg Loan 1, Dundee Medipark, DD2 1FD Dundee, United Kingdom

^d SINTEF Technology and Society, Department of Medical Technology, Olav Kyrres gate 9, MTF5, Trondheim, Norway

^e Amper Kliniken AG, Klinikum Dachau, Department of Clinical and Interventional Radiology, FUS-Center, Krankenhausstrasse 15, D-85221 Dachau, Germany

^f Sapienza University of Rome, Department of Radiological, Oncological and Pathological Sciences, V.le Regina Elena 324, 00180 Rome, Italy

ARTICLE INFO

Article history:

Received 1 May 2015

Revised 28 December 2015

Accepted 1 January 2016

Available online 15 January 2016

Keywords:

Workflow analysis

Focused ultrasound surgery

Workflow simulation

MRgFUS

High intensity focused ultrasound

ABSTRACT

Magnetic resonance guided focused ultrasound surgery (MRgFUS) has become an attractive, non-invasive treatment for benign and malignant tumours, and offers specific benefits for poorly accessible locations in the liver. However, the presence of the ribcage and the occurrence of liver motion due to respiration limit the applicability MRgFUS. Several techniques are being developed to address these issues or to decrease treatment times in other ways. However, the potential benefit of such improvements has not been quantified. In this research, the detailed workflow of current MRgFUS procedures was determined qualitatively and quantitatively by using observation studies on uterine MRgFUS interventions, and the bottlenecks in MRgFUS were identified. A validated simulation model based on discrete events simulation was developed to quantitatively predict the effect of new technological developments on the intervention duration of MRgFUS on the liver. During the observation studies, the duration and occurrence frequencies of all actions and decisions in the MRgFUS workflow were registered, as were the occurrence frequencies of motion detections and intervention halts. The observation results show that current MRgFUS uterine interventions take on average 213 min. Organ motion was detected on average 2.9 times per intervention, of which on average 1.0 actually caused a need for rework. Nevertheless, these motion occurrences and the actions required to continue after their detection consumed on average 11% and up to 29% of the total intervention duration. The simulation results suggest that, depending on the motion occurrence frequency, the addition of new technology to automate currently manual MRgFUS tasks and motion compensation could potentially reduce the intervention durations by 98.4% (from 256 h 5 min to 4 h 4 min) in the case of 90% motion occurrence, and with 24% (from 5 h 19 min to 4 h 2 min) in the case of no motion. In conclusion, new tools were developed to predict how intervention durations will be affected by future workflow changes and by the introduction of new technology.

© 2016 Elsevier Inc. All rights reserved.

1. Introduction

The non-invasive ablation of tumours in the human body is a goal that is becoming reality with the introduction of MRI-guided

focused ultrasound surgery (MRgFUS). In focused ultrasound surgery (FUS), a beam of acoustic energy is transmitted into the tissue of the human body by a FUS-transducer, and is concentrated in a focal point for about 15–45 s. Such a pulse is called a ‘sonication’ and firing such a pulse at a target spot is called ‘sonicating’. At the focal point, the tissue heats up to the point that it becomes necrotic, whereas outside the focal point, the tissue remains undamaged [1]. MRI is a valuable modality for target definition, intervention planning, and closed-loop control of the acoustic energy deposition during FUS. In addition, MRI provides accurate, real-time temperature maps. Such thermal feedback facilitates

* Corresponding author.

E-mail addresses: A.J.Loeve@tudelft.nl (A.J. Loeve), jumana.al-issawi@gmx.de (J. Al-Issawi), Fabiola.FG@gmail.com (F. Fernandez-Gutiérrez), Thomas.Langø@sintef.no (T. Langø), Jan.Strehlow@mevis.fraunhofer.de (J. Strehlow), Sabrina.Haase@mevis.fraunhofer.de (S. Haase), Matthias.Matzko@gmail.com (M. Matzko), Alessandro.Napoli@uniroma1.it (A. Napoli), A.Melzer@dundee.ac.uk (A. Melzer), J.Dankelman@tudelft.nl (J. Dankelman).

<http://dx.doi.org/10.1016/j.jbi.2016.01.001>

1532-0464/© 2016 Elsevier Inc. All rights reserved.

intervention monitoring, since it allows for the immediate evaluation of the temperature in the targeted volume, which helps to minimise the risk of damaging the adjacent tissues [2–4].

Over the last two decades, MRgFUS has become an attractive non-invasive treatment for both benign and malignant tumours. MRgFUS has been approved by the US Food and Drug Administration (FDA) for uterine fibroid treatment, and is in ongoing clinical or pre-clinical trial for the treatment of breast, liver, prostate, and brain cancer, and for the palliation of pain in bone metastasis [5,6]. There have been attempts to treat liver tumours with MRgFUS in pre-clinical trials [7,8] and in clinical trials [9,10]. MRgFUS enables the treatment of parts of the liver that are poorly accessible for conventional surgery, and may even reduce the need for conventional surgery and its accompanying risks. However, despite the potential benefits of MRgFUS, there are two major challenges to be overcome if it is to be broadly applied on the liver: the presence of the ribcage surrounding the liver, and the liver motion due to respiration (or coughing or sneezing).

The bone tissue of the ribs would absorb most of the acoustic energy, blocking the acoustic beam path towards liver tumours and causing unwanted, potentially damaging heating of the skin and ribs [11]. To avoid sending the acoustic energy through the ribs, several studies have focused on multiple-element ultrasonic transducers in which elements can be selectively switched on or off depending on their beam path towards a target in the liver [12–14]. Respiratory motion causes a cyclic shift in liver tumour position, resulting in healthy tissue rather than the tumour being heated if no compensation is made in the FUS beams over the breathing cycle. The liver movement can also induce motion artefacts in the MR and temperature maps [15]. Voluntary breath-holding, gating techniques, and controlled breathing during general anaesthesia have all been suggested to prevent organ movement during sonications [16]. Reference-less MR thermometry and active steering of the FUS beam have been used to compensate for organ motion [17–19].

MRgFUS procedures are currently rather time-consuming. Improvement of the time- and cost-efficiency of MRgFUS is sought in technological developments, including the automation of procedure planning and execution and the automation of image segmentation [14].

The authors were aware that in order to develop necessary technology and tools for MRgFUS on the liver and other moving organs, it is crucial to fully understand the workflow of MRgFUS. By identifying the bottlenecks in the current workflow it would be easier to properly improve and optimise the current MRgFUS procedures. Furthermore, if a quantitative estimate could be made of the benefits that can be obtained by introducing new technologies, it would be possible to focus research efforts more efficiently. Despite ongoing developments aimed at enabling MRgFUS for moving abdominal organs, neither detailed workflows of MRgFUS nor quantitative estimates of the potential benefits of new technology on the workflow could be found in the literature. Therefore, the aim of this study was:

- to estimate quantitatively the workflow improvements that can be achieved by the key technologies that are currently being developed for MRgFUS.

To do so, it was necessary to first:

- establish the detailed workflow of current clinical practice in MRgFUS,
- identify the bottlenecks in current clinical practice in MRgFUS, and
- build and validate a workflow simulation model for MRgFUS.

2. Methods

2.1. Workflow observations

As technologies required for enabling safe MRgFUS on the liver are still being developed, MRgFUS has not yet been cleared for liver treatments. The workflow of current clinical practice in MRgFUS was therefore determined through observations of the well-established MRgFUS treatment of uterine fibroid.

A working version flowchart ('observation flowchart') of the MRgFUS workflow was developed on the basis of observations and time registrations during:

- three uterine MRgFUS interventions in the Policlinico Umberto I, Rome, Italy,
- one uterine MRgFUS intervention in the Amper Klinikum, Dachau, Germany, and
- four iteration sessions with clinical experts (surgeons and interventional radiologists), clinical FUS experts and workflow experts within the consortium of the European FP7 "FUSIMO" project (www.fusimo.eu, accessed 13 March 2014).

The observation flowchart was used during 12 uterine MRgFUS intervention observations to make detailed registrations of the durations and occurrence frequencies of most actions and decision points described in the observation flowchart. These observation data were used to verify that the developed workflow agrees with clinical practice, and to obtain probability distributions for the workflow simulations that are described in Section 2.3. Six of those observations were conducted in the clinic in Rome, and six were conducted in the clinic in Dachau. Anonymous patient data, namely age, anamnesis, build, and names of the interventional radiologist and his support team, were gathered for each observation. These data were collected to assure that the patient group was reasonably homogeneous and to allow checking whether any potential workflow deviations were related to the patient demographics. Noticeable events or situations were noted during the observations and included in the data files. In order to support the observation data, a questionnaire was completed by the interventional radiologists to obtain estimates of the likelihood of specific events occurring.

Some actions and decision points described in the observation flowchart always followed automatically, and often instantly, after specific other decision points or actions and had such short durations that registering individual durations was infeasible and unnecessary. For such actions and decision points a duration of one second was used.

All observations and registrations were done by the same observer (author AJL). All observed MRgFUS interventions were uterine fibroid interventions performed by highly experienced interventional radiologists. All interventions were performed using ExA-plate (InSightec, Haifa, Israel) FUS equipment and software, further referred to as "the FUS-software". A preliminary ethics review was done at the departmental level and according to the applicable guidelines, the studies were exempt from a full ethics board review in either of the two hospitals. If the study is to be repeated later or elsewhere, a complete ethics review may be necessary.

Descriptive statistics were obtained from the observation data to identify bottlenecks in the MRgFUS workflow, and to discover which actions and phases in the workflow were the most time-consuming. For reasons of clarity and comprehensibility, in this report detailed quantitative results are given only on the phase levels and not on the level of individual actions or decision points.

2.2. Workflow phases

As it is unavoidable to refer to specific phases of the MRgFUS interventions in the description of the workflow simulations, a brief explanation of the major phases that are distinguished in MRgFUS interventions (Fig. 1) is provided here. The current MRgFUS workflow consists of eleven main phases:

Phase 1: Intake. The patient's history, clinical condition, complaints and suitability for MRgFUS are considered and discussed.

Phase 2: Pre-operative imaging. To support any decision making on indications, suitability and treatment approach, CT, MRI, and/or PET-CT scans may be acquired.

Phase 3: Pre-operative planning. A treatment plan can be prepared using the FUS-software prior to the actual day of the treatment.

Phase 4a: Setup. The MRI-room and the patient are prepared for the treatment.

Phase 4b: Patient positioning. The patient is positioned on the MRI-table such that there is an acoustic window (free field of view) for the FUS-transducer on the volumes of tissue that are to be sonicated ('regions of treatment').

Phase 5: Pre-therapy imaging. Detailed MR scans are acquired for use during the planning and execution of the treatment.

Phase 6a: Pre-therapy segmentation. Relevant structures are marked on the MR images to indicate where sonication energy should and should not go.

Phase 7: Sonication calibration. The FUS-transducer and the FUS-software system are calibrated to ensure accurate predictions of ultrasound propagation.

Phase 6b: Pre-therapy planning. The regions of treatment on the MR images are filled with planned sonications.

Phase 8: Treatment. Planned sonications are executed one by one, allowing for intermediate adjustments of the plan.

Phase 9: Post-therapy imaging. After sonicating the entire target volume, MR images are taken to check the treatment outcome.

2.3. Workflow simulations

The established detailed workflow was adapted for future liver treatments (liver flowchart). A detailed discrete events simulation ('DES') model was built in Delmia Quest modelling software (Dassault Systèmes S.A., Vélizy-Villacoublay, France) on the basis of the liver flowchart and the observation data gathered in the clinic in Dachau. The model was implemented according to the validated methods described by Fernandez-Gutierrez in [20], in which a complete list of all probability distributions used in the model is also provided.

Probability distributions for durations of actions and decision points that were not instant were obtained using the observation data and the software package EasyFit (MathWave, Dnepropetrovsk, Ukraine). The Anderson–Darling goodness-of-fit test was used ($\alpha = 0.05$) to determine the best fitting probability distributions [21]. It was assumed that duration distributions had a finite lower bound of zero.

A decision point was defined as static in the modelling software when the probabilities of each of the possible outcomes of the decision did not depend on the number of times that the decision point was executed with the same patient. These probabilities were simply programmed using 'if-then-else' statements and were based on the observation data. A decision point was defined as dynamic when the probabilities of each of the possible outcomes changed depending on the number of times that the decision point was executed. Because of the limited sample size in this study, a Markov chain model was used to model the outcome probabilities in dynamic decision points [22].

The number of sonications varies between patients and depends on the size of the treatment volume. The observation data could be roughly divided into a group of short interventions (39 sonications on average) and a group of long interventions (107 sonications on average). For the workflow simulations either a short or a long intervention was used, with a 50% probability for each. The number of sonications for a simulated intervention was modelled with a Poisson distribution with a mode of 39 sonications for short interventions and 107 sonications for long interventions.

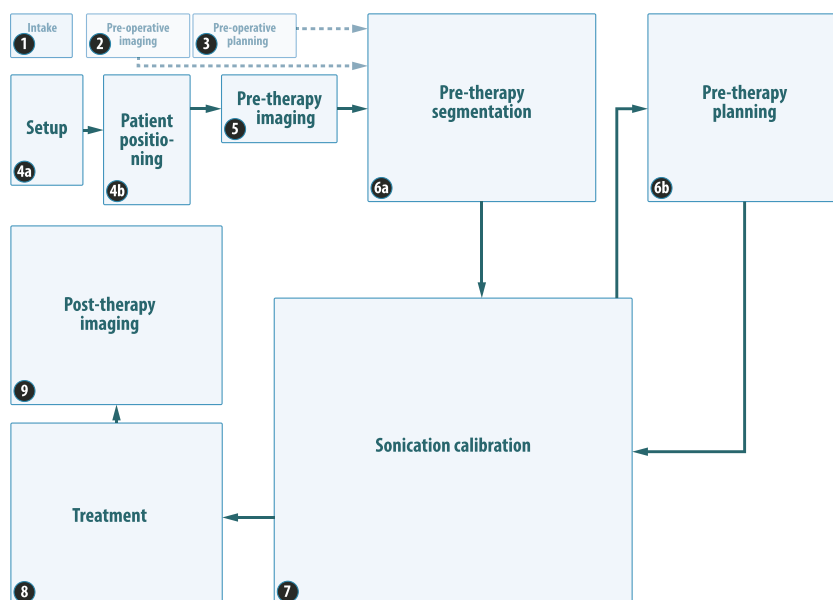


Fig. 1. Global phases describing the workflow in MRgFUS.

The workflow simulation model was validated by:

- (1) Observing the operational behaviour of the model through animation outputs of the simulation.
- (2) Confirming event validity by checking whether the occurrences and recurrences of events and decision points (loops) agreed with the observation data.
- (3) Confirming the internal validity through a variability analysis. For this, the simulation model was compared with the real system following the method for the Behrens–Fisher problem [23], for an unknown ratio of variance, using the Welch 90% confidence interval ('WCI'). Because of the large number of phases, actions and decision points, it was infeasible to conduct this check for each individual phase, action and decision point.

To calculate the WCI, batches of 100, 300, 1000, and 3000 simulations were executed, with each simulation containing 30 runs. The number of runs per simulation was chosen arbitrarily, but it was based on the suggestions given in the simulation software's manual and was sufficient to obtain results within an acceptable confidence interval. The WCI was calculated for each batch until a WCI was found that included zero, which is a necessary condition to validate the model against the real system.

The key technologies that are currently being developed for MRgFUS are aimed at reducing either procedure times or the effects of organ motion on the workflow. Simulations were therefore run to estimate the effect of organ motion on the workflow in five distinct scenarios:

- Scenario 1: **Current motion effect.** The MRgFUS procedure duration was determined for the established workflow in the situation in which no critical motion of the treatment volume occurs, in the situation in which critical motion of the treatment volume occurs in 90% of all sonications, and in all intermediate situations in steps of 10% motion occurrence.
- Scenario 2: **Automated segmentation.** For each amount of motion in Scenario 1, the procedure duration was determined but this time with the workflow improved as follows: the durations of actions regarding the segmentation of images (X2 in Phase 6a and X6 in Phase 9) were reduced to an average of 60 s. This mimics a workflow in which segmentation is done fully automatically by the FUS-software. This 60 s average duration was a conservative estimate, based on the authors' hands-on experiences with automated segmentation algorithms.
- Scenario 3: **Automated sonication.** For each amount of motion in Scenario 1, the procedure duration was determined but this time with the workflow improved as follows: in Phase 8, the Treatment Phase, the duration of X4 was set to zero (as sonication parameters will be adjusted instantly by the system), and the probabilities of having to wait for the MRI or the FUS system were reduced from 25% to 10%. This mimics a workflow in which the entire treatment plan is executed automatically. The reduction of the waiting time was chosen because the waiting time in current practice is often extended by a physician talking to his or her assistants while they were waiting. Furthermore, a subsequent sonication could only be fired after the cooling down per-

iod had passed to prevent surrounding tissue from overheating. The heating of surrounding tissue is expected to be limited by automatically calculating the optimal path of the sonication beam.

Scenario 4: **Combined effect.** For each amount of motion in Scenario 1, the procedure duration was determined but this time with the workflow improvements of both Scenario 2 and 3.

Scenario 5: **Motion compensation.** As in Scenario 4, but with the workflow further improved as follows: motion compensation technology was incorporated into the workflow, leading to 95% of all motion occurrences staying below critical levels. In this scenario, it was assumed that the motion compensation technology tracks the motion of the treatment volume and compensates for that motion by automatically and continuously steering the sonication beam to keep it focused on the targeted sonication spot [18]. Furthermore, the motion compensation technology disables individual FUS-transducer elements whenever necessary to avoid risk structures, such as ribs or air-filled organs [12]. The level of 95% was based on estimates of organ motion and the requirements expressed by expert interventional radiologists, and prototype demonstration results of systems currently under development [24]. As a result, the motion occurrences stayed within such bounds that the motion compensation technology is able to cope with that motion in 95% of all occurrences.

The number of simulation runs in each scenario was based on the smallest batch size for which the WCI was found.

3. Results

3.1. Workflow observations

The observed interventions were performed on women aged 22–51 years (AVG 39 years, STD 9.3 years). None of the patients was obese. One observation in the clinic in Rome was excluded from the analysis because the MRgFUS equipment failed early in the intervention and the remainder of that intervention had to be cancelled. As a result, six interventions in Dachau and five interventions in Rome were included in the analysis. No structural workflow differences were observed between the institutes or between patients. In one case, setting up the patient took significantly longer in one case than in the others because the patient was a bit corpulent and had an old subcutaneous lesion.

Fig. 2 shows a flowchart of the detailed workflow in current clinical practice in MRgFUS. Fig. 3 explains the symbols used in the flowchart. A walkthrough for the entire intervention is summarized below, with references to action and decision numbers given in square brackets:

Phase 4a: Setup. The MRI room is prepared, the MRI table is connected, and a pad of coupling gel is placed on the MRI-table; the patient is then brought into the MRI room [X1]. The patient lies face-down on the MRI-table, with the region of treatment approximately centred above the FUS-transducer. The patient is given a panic button to hold throughout the entire intervention. The patient is told to push the button whenever experiencing pain or anxiety, or having any urgent needs or questions.

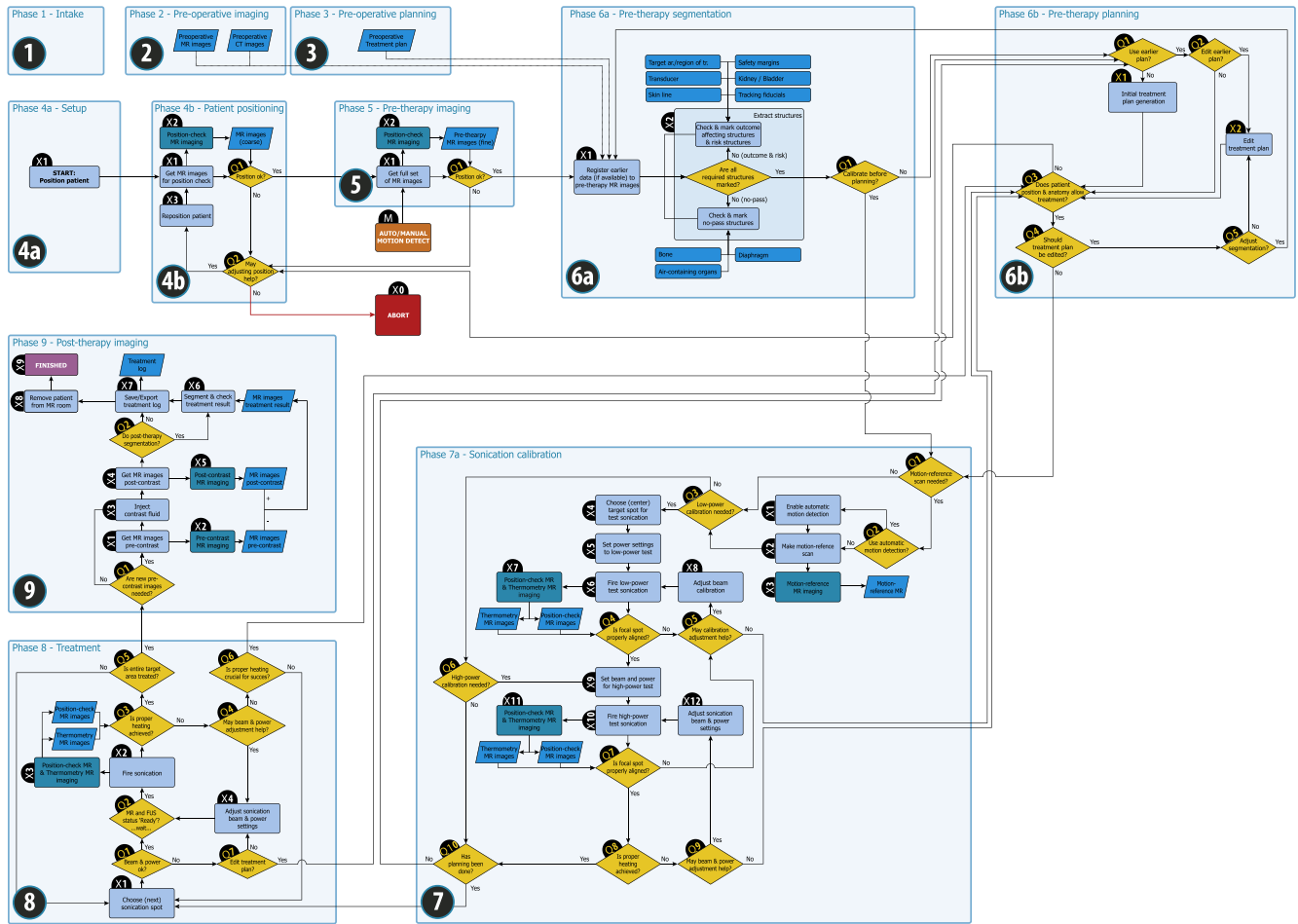


Fig. 2. Detailed flowchart of the workflow in MRgFUS. The symbols used in the figure, are explained in Fig. 3.

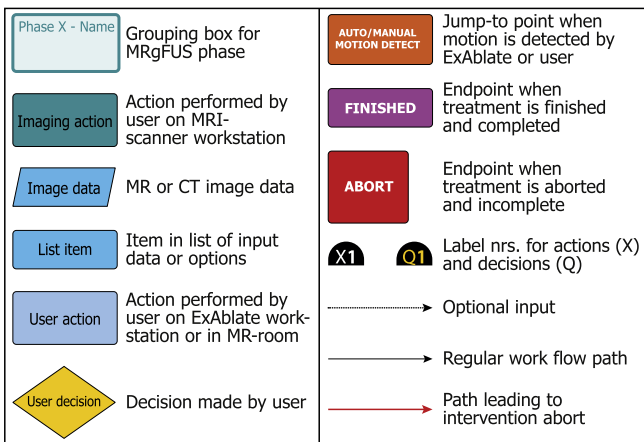


Fig. 3. Legend explaining the symbols used in Fig. 2.

Phase 4b: Patient positioning. A first set of fast, low-resolution MR images is made [X1, X2] to check whether there is a free window for the sonication beam to reach the entire region of treatment. If the patient position is not satisfactory [Q1], it is visually determined whether repositioning may help [Q2]. If so, the patient is repositioned [X3] and new images are made to check again. This process is repeated until the patient position is satisfactory [Q1] or the interventional radiologist decides that a free window cannot be obtained [Q2]. The latter may

happen when, for example, air-filled organs (intestines) are blocking the acoustic path and cannot be moved. In this case, the intervention is aborted [X0].

Phase 5: Pre-therapy imaging. After properly positioning the patient, a full set of high resolution sagittal, coronal, and transversal MR images are acquired [X1, X2]. The images must cover the region of treatment and all critical structures around it. Before continuing, it is checked once more whether the patient position allows sonication of the entire region of treatment [Q1]. If any problems are noticed, Phase 4b is re-entered. **Phase 6a: Pre-therapy segmentation.** If any prior imaging data are available, they can be registered to the newly acquired images [X1]. This is usually done when new images are made during the intervention after organ motion or whenever the interventional radiologist decides to make new images to confirm that motion did not occur. All relevant structures are marked on the MR images [X2]: the region of treatment, structures that must not be hit by the sonication beam, and structures that may affect the treatment [X2]. Furthermore, tracking fiducials are placed as a reference for both automated and manual motion tracking. Depending on the FUS-software version, either Phase 7 or 6b follows, with the former being forced first in the latest software versions.

Phase 7: Sonication calibration. During the first pass of Phase 7, or whenever organ motion has occurred [Q1], a motion-reference scan is made that serves as the reference situation for motion detection [X1, X2, X3]. Automatic motion detection is generally used [Q2], but under certain conditions it may be

disabled. During the first pass of Phase 7, or whenever significant patient repositioning or system parameters changes have occurred [Q3], a low-power calibration sonication is fired onto the centre of a region of treatment [X4 to X7] to check that the acoustic focal point occurs at the predicted location [Q4]. If there is a focal point mismatch, the calibration can be adjusted [Q5, X8] and checked again. Too thick skin layers or air-filled organs may cause unpredictable acoustic propagation, making proper focal point alignment difficult or even impossible. In such cases, it may be necessary to reposition the patient or even abort the intervention ['No' at Q5]. A high-power sonication is fired [X9 to X11] to check that focal point alignment persists with high sonication power [Q7] and that proper tissue heating is achieved [Q8]. Any necessary calibration adjustments can be made [Q9, X12] and planning has to be done [Q10] before continuing to Phase 8.

Phase 6b: Pre-therapy planning. At the first pass of Phase 6b and if no pre-operative plan was loaded in Phase 6a [Q1], a new treatment plan is made [X1]. Regions of treatment are automatically or manually filled with planned sonications, and adjusted whenever necessary. The FUS-software establishes for each planned sonication whether the sonication beam would hit any no-pass or risk structures, and then indicates whether that sonication can be achieved. Whenever an earlier plan is available from pre-operative planning or from earlier during the intervention, the plan can be edited if necessary [Q2, Q4, X2]. If the patient position or the segmentation should be changed [Q3, Q5], for example after organ motion, Phase 4b or 6a can be re-entered.

Phase 8: Treatment. Planned sonications are executed one by one [X1], each time selected manually or in the order suggested by the FUS-software. The interventional radiologist checks that the beam and power settings for the sonication are set properly by the FUS-software, and may decide to adjust the settings [Q1, Q7, X4] based on experience or after firing a sonication that proved to be of too low power [Q4]. The FUS-software allows a subsequent sonication to be fired [Q2, X2] only after the MR scanner and the FUS-probe are ready for it. Regular and thermometry MR images are shown during and after the sonication [X3], allowing the interventional radiologist to watch for organ motion and to evaluate the sonication result [Q3]. If sonication at a specific location does not achieve the intended tissue heating, even after increasing the sonication power [Q4], it may be decided to adjust the plan or to continue with the next sonication spot whenever the targeted spot is not crucial for the treatment to succeed [Q6]. Phase 8 continues until sufficient sonications have been successfully executed to ablate the entire target volume, which is the total of all regions of treatments [Q5].

Phase 9: Post-therapy imaging. If organ motion occurred, or is suspected after the latest set of scans (Phase 5) [Q1], a new set of MR images are made [X1, X2] before administering contrast fluid to the patient [X3]. After making post-contrast MR images [X4, X5], the pre- and post-contrast MR images are subtracted from each other to visualize, segment, and measure the volume of successfully ablated tissue [X6]. This can be done immediately or after the intervention [Q2]. Log files of the intervention are exported and/or saved for archiving and review [X7]. The patient is then removed from the MR room [X8], at which point the intervention ends.

Action M: Auto/Manual motion detection. At any instant during the intervention, the process can be instantly paused if the system detects any motion of the target organ or any marked structures around it. At this instant, the entire process steps out to Action M. This safety measure prevents accidentally damaging tissue outside the region of treatment. The pausing

function can be invoked by the interventional radiologist by clicking a stop button in the FUS-software or by hitting a hardware stop button on top of the FUS console directly in front of him. A pause may also be invoked by the patient by pressing the panic button. Whenever the system is paused, any active sonication is immediately aborted and the MR scanner stops scanning. After assessing the suspected organ motion or other irregularity, the interventional radiologist can start therapy again. It must then be decided whether to continue from Phase 5-X1 (in the case of motion or suspected motion) or from the step-out point (if no motion occurred).

Table 1 lists the mean durations for all intervention phases, as well as recurrence frequencies for all intervention phases and all events that invoked a system pause. **Table 1** also shows how many of the motion alarms (automatic and manual) appeared to really be caused by organ motion, and thus were considered relevant, after detailed assessment by the interventional radiologist.

The total intervention time was 214 min on average, with the shortest intervention taking only 112 min and the longest taking 403 min. About 56% of the intervention time was spent on the actual treatment (Phase 8). About 12% of the remaining time was spent on pre-therapy imaging (Phase 5), and another 9% on post-therapy imaging (Phase 9). Patient positioning generally took about 3% of the intervention time and was only done prior to the rest of the intervention. Once the patient was properly positioned, repositioning was never necessary, even if organ motion had occurred. **Fig. 4** shows for all observed interventions the intervention times against the number of sonications. Although the shortest intervention also had the least sonications, the longest intervention had 86 sonications and lasted longer than the two interventions that had 96 and 145 sonications, respectively.

Motion detection led to the system being halted by the system on average 1.5 times and by the interventional radiologist on average 1.4 times. In general, only one in three motion detections appeared to be caused by actually relevant organ motion. Whenever organ motion was detected, Phases 5 to 8 generally all had to be re-entered in the order shown in **Fig. 2**. Whenever the detected motion was small enough or appeared to be a false alarm (which can happen if the organ moves and then moves back to its original position), sometimes new MR images were acquired in Phase 5 as a check and then the intervention was continued. On average, about 11% of the total intervention time was spent on re-entering already passed phases after motion detections.

Patients pushed the panic button on average 2.7 times due to pain and 0.8 times for other reasons. Four patients did not push the panic button. One patient pushed the panic button 14 times because of mild pain in the back or legs (the region of treatment was close to the spine) and four times because of nausea, cold, thirst or involuntary pushing due to a slight tremor. In two interventions the interventional radiologist pushed the stop button once because the MR thermometry images shown during sonication (Phase 8–X3) raised suspicion of excessive heating in the vicinity of a risk structure. A system warning popped up twice; once because of suspected potentially critical acoustic reflections and once because of a software error. In both cases the intervention was continued after carefully reviewing all system settings, and the system warning did not reoccur.

3.2. Workflow simulations

Fig. 5 shows the implemented MRgFUS workflow simulation model. Probability distributions could be determined for all action and decision points durations. The model was verified against the observation data and the Welch 90% confidence interval ('WCI') was found when running the batch of 3000 simulations to be

Table 1
Descriptive statistics of workflow observation data, listing phase durations, phase occurrence frequencies, and motion occurrences. Phase durations and phase occurrence frequencies are given as totals per phase as well as split per phase for the first pass of the phase and for the recurrent passes, which are passes that occur after Phase 8 has been entered for the first time. Recurrent passes are made whenever Phase 8 has to be exited due to any kind of alarm, motion detection, panic button push or user-evoked system halt.

	Durations (min)		% Mean Phase Duration vs. Intervention Time	Occurrence Frequencies	
	Mean	St Dev		Mean	St Dev
Phase 4a	10.6	5.7	5.0%	1.0	0.0
Phase 4b	6.5	4.8	3.1%	1.0	0.0
First Pass	6.5	4.8	3.1%	1.0	0.0
Recurrent Passes	0.0	0.0	0.0%	0.0	0.0
Phase 5	25.4	13.1	11.9%	2.5	1.2
First Pass	15.1	9.8	7.1%	1.0	0.0
Recurrent Passes	10.4	8.7	4.9%	1.5	1.2
Phase 6a	17.7	9.9	8.3%	2.5	1.2
First pass	11.7	7.5	5.5%	1.2	0.6
Recurrent Passes	6.0	5.5	2.8%	1.3	1.1
Phase 6b	4.8	8.7	2.3%	2.5	2.0
First Pass	2.5	5.3	1.2%	1.2	0.6
Recurrent Passes	2.4	4.0	1.1%	1.3	1.7
Phase 7	14.3	5.8	6.7%	2.3	1.1
First Pass	11.3	4.8	5.3%	1.0	0.0
Recurrent Passes	3.0	4.6	1.4%	1.3	1.1
Phase 8	119.8	93.4	56.1%	3.2	1.9
First Pass	60.5	93.2	28.4%	1.2	0.6
Recurrent Passes	59.2	61.6	27.7%	2.0	1.8
Phase 9	18.7	9.4	8.7%	1.0	0.0
Sum of Phases	213.1	110.3			
Total Intervention	213.5	107.2			
Sum of Recurrent Passes of Phases 4b - 7a	21.7	17.3			
% Recurrents vs. Intervention Time	11%	10%			

Intervention Interruptions	Occurrence Frequencies	
	Mean	St Dev
Motion Detection by System	1.5	1.6
Motion Detection by User	1.4	2.6
Motion Requiring Rework	1.0	1.0
Panic Button: Patient Pain	2.7	4.3
Panic Button: Other Reason	0.8	1.4
Stop by User	0.2	0.4
Stop by System	0.2	0.4

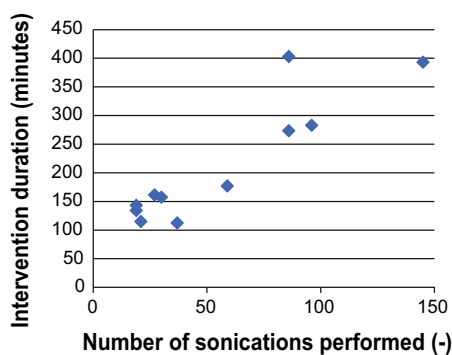


Fig. 4. Intervention duration versus number of executed sonications (including retried sonications).

[1064, –4228]. Therefore, 30 runs were simulated for each scenario with 3000 simulation runs per patient to ensure that the results would be within the WCI.

Fig. 6 shows the mean total intervention duration versus the motion occurrence percentage for all simulated scenarios. The mean intervention duration increased exponentially with the motion occurrence, namely from 3 h 57 min in the case of having no motion, to 256 h 5 min in the case of detecting motion in 90%

of all sonications. Introducing automated segmentation (Scenario 3) gave a significantly greater reduction of the intervention duration than was achieved by introducing automated sonication (Scenario 2). Adding motion compensation technology (Scenario 5) gave the greatest reduction of the intervention duration, that is, from 256 h 5 min to 4 h 4 min in the case of 90% motion occurrence, which is a 98.4% decrease. In the case of no motion, the achieved improvement was still 24%. Further details about the simulation model, including statistical distributions and confidence intervals for each of the scenarios, are provided in Appendix A.

4. Discussion

This present study was the first to produce a full and detailed description of the workflow in MRgFUS. The durations and occurrence frequencies of all relevant phases, actions and decisions were obtained, providing insight into the major bottlenecks and points for improvement in MRgFUS. No differences in the workflow structure were found between the two hospitals where the observations were conducted. All observed interventions fitted the developed workflow description. The simulation model that was developed and validated against observation data proved to be an efficient means to obtain quantitative predictions for the effect of changes in the MRgFUS workflow on intervention duration.

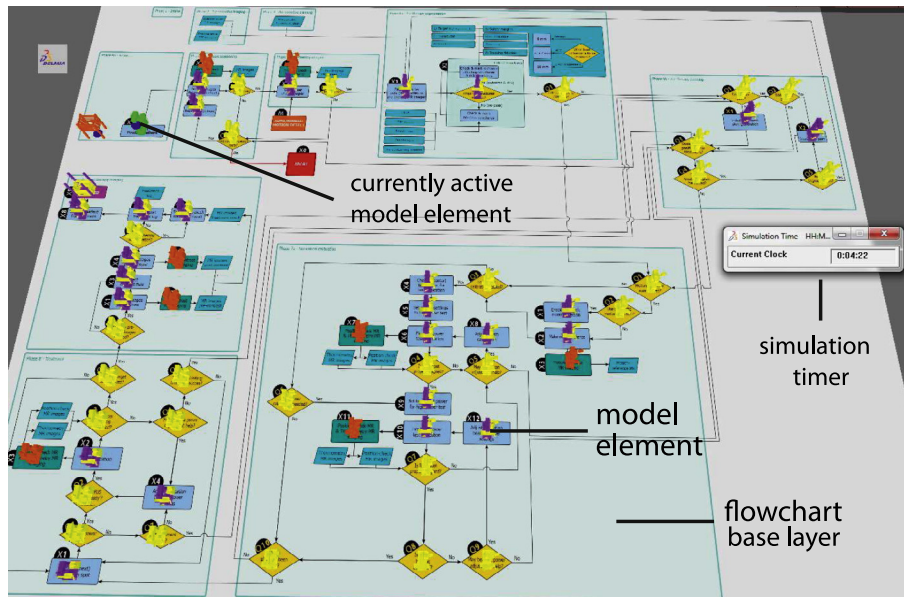


Fig. 5. Screenshot of the Delmia Quest workflow simulation model that was implemented, verified, validated and used to predict the effects of future changes to the MRgFUS workflow.

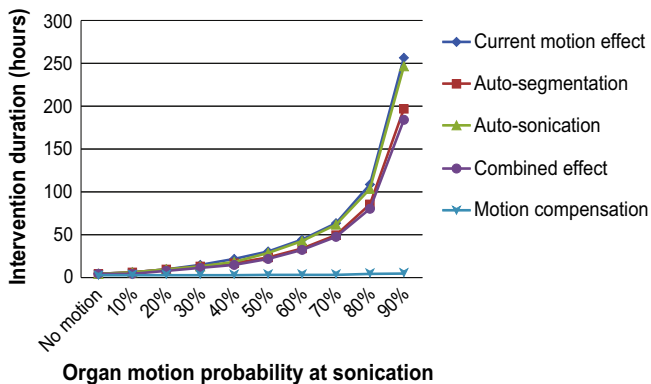


Fig. 6. Predicted mean intervention duration versus probability of motion occurrences during the sonications. Each data point is the mean of 3000 simulations of 30 patients each.

The observed MRgFUS interventions were all uterine fibroid treatments, a well-established kind of intervention. Yet, even in these interventions in which breathing motion of organs only actually occurs once on average, organ motion and the actions required to continue after its detection or suspicion still consumed on average 11% and up to 29% of the entire intervention duration. This implies that even in current MRgFUS on target volumes that generally do not move too much, care should be taken to prevent as much organ motion as possible. Motion might be limited by careful instruction of the patient, properly securing the patient to the MRI table with respect to the FUS transducer, suppressing coughing, and limiting bladder filling during the intervention.

Preparing the MRI room, positioning the patient, creating the treatment plan after segmentation of the MR images, and calibrating the MRgFUS system were generally fast processes. These four phases together took on average only 17% of the intervention duration. In a few cases, the calibration of the system took a relatively long time because of the presence of relatively thick layers of skin and fat between the ultrasound transducer and the region of treatment. These tissue layers caused deflections of the ultrasound beam and required the patient to be repositioned.

The results seem to suggest a linear relationship exists between intervention duration and the number of sonications required to ablate the entire region of treatment. However, as the minimum intervention duration will always incorporate Phases 4a to 7, it can be reduced only to a limited extent.

Image segmentation took on average about 18 min in Phase 6a and about 2 min when calculating the ablated volume in Phase 9. The simulation results suggest that the total intervention duration could be reduced by 2% in current interventions by using automated segmentation (Fig. 6), assuming segmentation times of up to 60 s. In cases where organ motion occurs, the intervention duration reduction can be as large as 24% due to the need to make new images and to adjust the segmentation after each motion occurrence.

The spot-by-spot sonication currently used in clinical practice is a rather slow process. The FUS-transducer must be positioned for each sonication, after which sonication is performed. A waiting period (often up to a minute) is then invoked to allow the tissue in and around the sonication beam to cool down. When automating sonication to perform batch sonications while taking heat spreading into account, intervention durations may drop by 15% in cases when no motion occurs (Fig. 6). In high motion occurrence cases, however, the reduction is only 4%, probably to be explained because series of continuously performed sonications are split into sessions of a few sonications, or even just a single sonication, due to the motion.

In current MRgFUS on target volumes that do not move too much, clinical practice may benefit most from speeding up the segmentation and sonication processes. Yet, for MRgFUS on moving abdominal organs, motion compensation is the essential key to feasibility. Due to the lack of such techniques in current clinical practice, no physician would consider treating moving abdominal organs with the currently available equipment, as their limitations are obvious. However, the current results are the first to provide quantitative data on the relationship between organ motion and intervention duration, and on the improvements that could be achieved with new technology.

The observation data showed that motion of the treatment volume largely affects the intervention duration. The simulation data showed that intervention duration increases ever more rapidly

Table A.1

Statistical distributions and parameters corresponding to each stage collected, where α , m and σ are shape parameters, and β and μ are scale parameters describing the selected distribution. If (*) is placed behind the distribution name, the null hypothesis was rejected on A–D, but that distribution was selected based on P–P curves and previous literature experience.

Event			Distribution	Parameters
Phase	Action	Decision		
4a	X1	Q1 Q2	Lognormal	$\mu = 6.02, \sigma = 0.73, \text{Mean} (\pm\text{SD}) = 538.17 (\pm 454.27)$
	X1		Lognormal	$\mu = 3.95, \sigma = 0.95, \text{Mean} (\pm\text{SD}) = 80.159 (\pm 93.683)$
	X3		Gamma	$\alpha = 0.88, \beta = 84.25$
			Gamma	$\alpha = 1.25, \beta = 12.21$
5	X1	Q1	Lognormal	$\mu = 4.00, \sigma = 1.54, \text{Mean} (\pm\text{SD}) = 178.77 (\pm 559.12)$
			Triangular	$\mu = 5.97, \sigma = 0.63, \text{Mean} (\pm\text{SD}) = 480.24 (\pm 336.86)$ $m = 30, a = 0, b = 58.36$
6a	X2		Lognormal	$\mu = 5.44, \sigma = 0.92, \text{Mean} (\pm\text{SD}) = 350.83 (\pm 404.99)$
	X3		Gamma	$\alpha = 1.51, \beta = 4.17$
7a	X4	Q4 Q8	Lognormal	$\mu = 1.44, \sigma = 0.79, \text{Mean} (\pm\text{SD}) = 5.80 (\pm 5.43)$
	X5		Gamma	$\alpha = 1.37, \beta = 16.95$
	X6		Triangular	$m = 152, a = 0, b = 152$
	X7		Weibull	$\alpha = 1.28, \beta = 78.86, \gamma = 0, \text{Mean} (\pm\text{SD}) = 73.05 (\pm 57.44)$
	X8		Gamma	$\alpha = 1.05, \beta = 15.86$
	X9		Lognormal	$\mu = 3.09, \sigma = 1.33, \text{Mean} (\pm\text{SD}) = 52.81 (\pm 116.17)$
	X10		Gamma	$\alpha = 24.96, \beta = 2.82$
	X11		Gamma	$\alpha = 17.80, \beta = 3.44$
			Gamma	$\alpha = 1.13, \beta = 11.45$
			Lognormal	$\mu = 1.53, \sigma = 1.62, \text{Mean} (\pm\text{SD}) = 17.20 (\pm 61.37)$
8	X1	Q1	Lognormal	$\mu = 3.18, \sigma = 0.82, \text{Mean} (\pm\text{SD}) = 33.82 (\pm 33.12)$
	X2		Gamma (*)	$\alpha = 16.44, \beta = 3.52$
	X3		Gamma (*)	$\alpha = 9.76, \beta = 4.54$
	X4		Lognormal	$\mu = 2.88, \sigma = 1.26, \text{Mean} (\pm\text{SD}) = 39.40 (\pm 77.55)$
9	X1		Lognormal (*)	$\mu = 1.67, \sigma = 1.12, \text{Mean} (\pm\text{SD}) = 9.98 (\pm 15.92)$
	X3		Lognormal	$\mu = 6.22, \sigma = 0.42, \text{Mean} (\pm\text{SD}) = 550.61 (\pm 241.78)$
	X4		Gamma	$\alpha = 11.72, \beta = 9.89$
	X8		Gamma	$\alpha = 18.29, \beta = 20.58$
			Lognormal	$\mu = 5.90, \sigma = 0.58, \text{Mean} (\pm\text{SD}) = 433.32 (\pm 276.65)$

with increasing motion occurrences. The outcome that patients would have to be treated for more than 10 continuous days (256 h:05 m) in the case of 90% motion occurrence (Fig. 6) clearly shows that without motion compensation or motion avoidance, MRgFUS can never be conducted safely on moving organs.

One of the most common ways to handle abdominal organ motion during treatments is to use a non-image based technique like respiratory gating. However, respiratory gating generally increases treatment time, as demonstrated in controlled apnoea on anesthetized pigs [8,10]. Motion modelling outperforms the gating approach [25], but requires tracking sensors to be attached to the patient. De Senneville and colleagues [15] proposed an image-based motion correction approach that generates, during an initial learning phase, an atlas of motion fields based on magnitude data of temperature-sensitive MR acquisitions, that is then used to correct the target position. Finally, assuming periodic motion, the focal point position for the next sonication cycle is estimated. The method can compensate for liver deformations caused by the periodic breathing motion, but cannot handle the non-

periodic deformations due to breathing and drift caused by intestinal activity (peristalsis) or muscle relaxation [26]. Although MR imaging can provide motion estimates with a high spatial resolution, it is difficult in practice to acquire online 3D isotropic images because of technical limitations, spatial and temporal resolution trade-offs, and the low signal-to-noise ratio associated with fast 3D acquisition sequences [27]. Moreover, the time duration between the actual target displacement and the availability of the motion information from MR data are not negligible [28]. Hence, slow MR data acquisition reduces the reliability of the target location when using MR information-based real-time motion compensation.

A first attempt at ultrasound-based motion tracking during MRgFUS was reported in phantoms undergoing periodic and rigid motion of small amplitude [28]. Continuous 1D ultrasound echo detection in a direction parallel to the main axis of motion was used. This setup is not suitable for clinical application, as the external ultrasound imaging probe cannot send beams parallel to the axis of respiratory motion. Moreover, the local motion in the liver

Table A.2

The 95% confidence intervals (in hours) for each of the scenarios analysed through the simulating model. Average values can be seen in Fig. 6.

Motion occurrence	Current workflow (simulation)	Automated segmentation	Automated sonication	Combined	Motion compensation
No motion	[3.90, 3.99]	[3.82, 3.92]	[3.31, 3.40]	[3.25, 3.32]	[3.25, 3.32]
10%	[6.72, 6.92]	[5.90, 6.08]	[5.90, 6.08]	[5.14, 5.31]	[3.31, 3.40]
20%	[10.00, 10.35]	[8.51, 8.79]	[9.30, 9.60]	[7.78, 8.02]	[3.38, 3.47]
30%	[14.42, 14.89]	[11.79, 12.22]	[13.50, 13.98]	[10.82, 11.15]	[3.46, 3.55]
40%	[20.62, 21.25]	[16.41, 16.94]	[16.41, 16.94]	[15.24, 15.77]	[3.58, 3.67]
50%	[29.02, 30.07]	[22.48, 23.21]	[27.22, 28.18]	[21.46, 22.21]	[3.67, 3.76]
60%	[41.47, 42.87]	[32.05, 33.14]	[40.22, 41.75]	[30.74, 31.85]	[3.73, 3.83]
70%	[62.43, 64.53]	[48.30, 50.02]	[61.36, 63.69]	[46.41, 48.23]	[3.81, 3.91]
80%	[106.50, 110.20]	[82.61, 85.42]	[103.00, 106.42]	[78.72, 81.51]	[3.99, 4.10]
90%	[250.99, 261.19]	[191.44, 197.53]	[242.32, 250.53]	[181.31, 187.43]	[4.02, 4.13]

varies spatially, and a 1D measurement would not suffice. Truly simultaneous ultrasound and MR imaging has only recently been reported in the literature [14,29–33]. Most of these studies involved the use of 2D ultrasound simultaneously with MR, whereas Tretbar et al. [32] used a dual plane ultrasound imaging transducer to enable a wider view deep inside the organs, by allowing beam steering over large angles. The consistent limitation of these studies was that out-of-plane motion could not be accounted for, as no multi-planar or 4D ultrasound was applied. 3D volumetric imaging is more suitable than 2D planar imaging for tracking motion in all directions.

Increasing interest is being shown in dynamic imaging for motion tracking. Dynamic imaging enables capturing the 3D deformation of the target volume and helps to plan sonications without having to assume periodic motion. 4D MR imaging has been used to generate models based on population studies [34,35] and can also be used to generate patient-specific models in preparation for an intervention.

The broad applicability of the observation data from this study may be limited because only 11 interventions were included. Each observation took half a day up to one day of continuous, manual registration of events, and several extra days were spent in the MR-rooms because about 30% of all interventions were cancelled by patients for various reasons. However, the experts who performed the interventions confirmed that the total dataset was a good representation of their everyday clinical practice. To gather more data, automated acquisition and analysing systems that register all relevant events during an intervention and automatically derive a workflow from the data would be of great use. Such systems are being developed for minimal invasive surgery [36–38], but are not yet available for MRgFUS.

A further limitation may be that the ExAblate MRgFUS system was used for all interventions. According to the physicians who took part in this study, however, the workflow for the ExAblate MRgFUS system is quite similar to that of the systems of other major vendors. Nevertheless, future studies will have to show the extent to which the developed workflow description and model apply when using other MRgFUS systems.

The estimated changes of the duration of specific workflow steps introduced by using automated segmentation, automated sonication, and motion compensation, were partly based on rough estimates. This was the best that could be done without having the actual future technology available to measure its effects. However, the simulation model allows one to easily adapt these estimates as well as any other parameters in the model. Therefore, the simulation model is a valuable tool to estimate the effect of any future change to the workflow of MRgFUS, and it may be used in the future for design optimisation of new MRgFUS technologies. For example, one could use the developed simulation model to check how different concepts of compensating and/or tracking motion would influence the workflow and intervention times.

The observed interventions were all uterine interventions and it is yet to be investigated whether the established workflow is representative of other MRgFUS interventions. However, during the pilot studies and in between uterine interventions, several MRgFUS treatments of bone lesions were observed. These additional observation data showed that the workflow itself did not change, even though the durations of individual phases could be quite different.

5. Conclusion

The detailed workflow of current clinical practice in MRgFUS was established, on the basis of observations of uterine MRgFUS interventions. Organ motion appeared to be the major prolonging factor of the intervention duration. Workflow simulations con-

firmed that with increasing motion occurrences, the intervention duration increases so rapidly that MRgFUS is clearly infeasible for treating moving abdominal organs with the currently available technology. The results further showed that automated segmentation, automated sonication, and motion compensation are technologies that will not only greatly reduce intervention durations, but are also expected to make feasible MRgFUS on moving abdominal organs. The observation data, the established workflow, and the developed simulation model have resulted in useful tools to predict how intervention durations will be affected by future workflow changes and by the introduction of new technology.

Acknowledgments

The authors would like to thank all MRgFUS team members in the clinics in Dachau and Rome for their hospitality and patience during the long days that parts of their work spaces were occupied by the author doing the observations, and Mrs. M.H.N. van Velzen for her help in processing and analysing the data. This work is funded by the European Union 7th Framework Program (FP7/2007–2013) grant agreement no.270186 (FUSIMO).

Appendix A

See Tables A.1 and A.2.

References

- [1] K. Fischer, W. Gedroyc, F.A. Jolesz, Focused ultrasound as a local therapy for liver cancer, *Cancer J.* 16 (2010) 118–124.
- [2] S.L. Hokland, M. Pedersen, R. Salomir, B. Quesson, H. Stødkilde-Jørgensen, C.T. W. Moonen, MRI-guided focused ultrasound: methodology and applications, *IEEE Trans. Med. Imaging* 25 (2006) 723–731.
- [3] S.A. Sapareto, W.C. Dewey, Thermal dose determination in cancer therapy, *Int. J. Radiat. Oncol. Biol. Phys.* 10 (1984) 787–800.
- [4] V. Rieke, K.B. Pauly, MR thermometry, *J. Magn. Reson. Imaging* 27 (2008) 376–390.
- [5] F.A. Jolesz, MRI-guided focused ultrasound surgery, in: *Annual Review of Medicine*, vol. 60, ed, 2009, pp. 417–430.
- [6] K. Hynynen, MRI-guided focused ultrasound treatments, *Ultrasonics* 50 (2010) 221–229.
- [7] F.A. Jolesz, K. Hynynen, N. McDannold, D. Freundlich, D. Kopelman, Noninvasive thermal ablation of hepatocellular carcinoma by using magnetic resonance imaging-guided focused ultrasound, *Gastroenterology* 127 (2004) S242–S247.
- [8] D. Kopelman, Y. Inbar, A. Hanannel, D. Freundlich, D. Castel, A. Perel, et al., Magnetic resonance-guided focused ultrasound surgery (MRgFUS): Ablation of liver tissue in a porcine model, *Eur. J. Radiol.* 59 (2006) 157–162.
- [9] W.M. Gedroyc, New clinical applications of magnetic resonance-guided focused ultrasound, *Top. Magn. Reson. Imaging* 17 (2006) 189–194.
- [10] A. Okada, T. Murakami, K. Mikami, H. Onishi, N. Tanigawa, T. Marukawa, et al., A case of hepatocellular carcinoma treated by MR-guided focused ultrasound ablation with respiratory gating, *Mag. Reson. Med. Sci.* 5 (2006) 167–171.
- [11] S.E. Jung, S.H. Cho, J.H. Jang, J.Y. Han, High-intensity focused ultrasound ablation in hepatic and pancreatic cancer: complications, *Abdom. Imaging* 36 (2011) 185–195.
- [12] J. Civalo, R. Clarke, I. Rivens, G. ter Haar, The use of a segmented transducer for rib sparing in HIFU treatments, *Ultrasound Med. Biol.* 32 (2006) 1753–1761.
- [13] B. Quesson, M. Merle, M.O. Köhler, C. Mougnot, S. Roujol, B.D. De Senneville, et al., A method for MRI guidance of intercostal high intensity focused ultrasound ablation in the liver, *Med. Phys.* 37 (2010) 2533–2540.
- [14] J.W. Jenne, T. Preusser, M. Günther, High-intensity focused ultrasound: principles, therapy guidance, simulations and applications, *Z. Med. Phys.* 22 (2012) 311–322.
- [15] B.D. De Senneville, C. Mougnot, C.T.W. Moonen, Real-time adaptive methods for treatment of mobile organs by MRI-controlled high-intensity focused ultrasound, *Magn. Reson. Med.* 57 (2007) 319–330.
- [16] I. Suramo, M. Paivansalo, V. Myllyla, Cranio-caudal movements of the liver, pancreas and kidneys in respiration, *Acta Radiol. – Series Diagnosis* 25 (1984) 129–131.
- [17] V. Rieke, A.M. Kinsey, A.B. Ross, W.H. Nau, C.J. Diederich, G. Sommer, et al., Referenceless MR thermometry for monitoring thermal ablation in the prostate, *IEEE Trans. Med. Imaging* 26 (2007) 813–821.
- [18] A.B. Holbrook, P. Ghanouni, J.M. Santos, C. Dumoulin, Y. Medan, K.B. Pauly, Respiration based steering for high intensity focused ultrasound liver ablation, *Magn. Reson. Med.* 71 (2014) 797–806.

- [19] S. Braunewell, M. Günther, T. Preusser, Toward focused ultrasound liver surgery under free breathing, *Crit. Rev. Biomed. Eng.* 40 (2012) 221–234.
- [20] F. Fernández-Gutiérrez, Workflow analysis, modelling and simulation for improving conventional and MRI-guided vascular interventions, PhD Thesis, Institute for Medical Science and Technology, Division of Imaging and Technology, College of Medicine Dentistry and Nursing, University of Dundee, Dundee, Schotland, 2014.
- [21] G.A. Wainer, *Discrete-Event Modeling and Simulation: A Practitioner's Approach*, first ed., CRC Press, London, UK, 2009.
- [22] D. Sirl, Markov chains: an introduction/review, in: *MASCOS Workshop on Algebraic Dynamics*, ed, University of New South Wales, Sydney, Australia, 2005.
- [23] H. Scheffe, Practical solutions of the Behrens–Fisher problem, *J. Am. Stat. Assoc.* 65 (1970) 1501–1508.
- [24] M. Schwenke, J. Strehlow, S. Haase, J. Jenne, C. Tanner, T. Lango, et al., An integrated model-based software for FUS in moving abdominal organs, *Int. J. Hyperther.* 31 (May 2015) 240–250.
- [25] G.S. Mageras, E. Yorke, Deep inspiration breath hold and respiratory gating strategies for reducing organ motion in radiation treatment, *Semin. Radiat. Oncol.* 14 (2004) 65–75.
- [26] M. Von Siebenthal, G. Székely, U. Gamper, P. Boesiger, A. Lomax, P. Cattin, 4D MR imaging of respiratory organ motion and its variability, *Phys. Med. Biol.* 52 (2007) 1547–1564.
- [27] M. Ries, B.D. De Senneville, S. Roujol, Y. Berber, B. Quesson, C. Moonen, Real-time 3D target tracking in MRI guided focused ultrasound ablations in moving tissues, *Magn. Reson. Med.* 64 (2010) 1704–1712.
- [28] P.L. De Oliveira, B.D. De Senneville, I. Dragonu, C.T.W. Moonen, Rapid motion correction in MR-guided high-intensity focused ultrasound heating using real-time ultrasound echo information, *NMR Biomed.* 23 (2010) 1103–1108.
- [29] D.A. Feinberg, D. Giese, D.A. Bongers, S. Ramanna, M. Zaitsev, M. Markl, et al., Hybrid ultrasound MRI for improved cardiac imaging and real-time respiration control, *Magn. Reson. Med.* 63 (2010) 290–296.
- [30] A.M. Tang, D.F. Kacher, E.Y. Lam, K.K. Wong, F.A. Jolesz, E.S. Yang, Simultaneous ultrasound and MRI system for breast biopsy: compatibility assessment and demonstration in a dual modality phantom, *IEEE Trans. Med. Imaging* 27 (2008) 247–254.
- [31] V. Auboiroux, L. Petrusca, M. Viallon, T. Goget, C.D. Becker, R. Salomir, Ultrasonography-based 2D motion-compensated HIFU sonication integrated with reference-free MR temperature monitoring: a feasibility study ex vivo, *Phys. Med. Biol.* 57 (2012) N159–N171.
- [32] S.H. Tretbar, H.J. Hewener, D. Speicher, T. Barthscherer, A. Bongers, J.W. Jenne, et al., MR-compatible ultrasound research platform for motion tracking to reduce motion induced artifacts in MR imaging, in: *2013 IEEE International Ultrasonics Symposium, IUS 2013, Prague, 2013*, pp. 553–556.
- [33] M. Viallon, S. Terraz, J. Roland, E. Dumont, C.D. Becker, R. Salomir, Observation and correction of transient cavitation-induced PRFS thermometry artifacts during radiofrequency ablation, using simultaneous Ultrasound/MR imaging, *Med. Phys.* 37 (2010) 1491–1506.
- [34] P. Arnold, F. Preiswerk, B. Fasel, R. Salomir, K. Scheffler, P.C. Cattin, 3D organ motion prediction for MR-guided high intensity focused ultrasound, in: *Medical Image Computing and Computer-Assisted Intervention: MICCAI ... International Conference on Medical Image Computing and Computer-Assisted Intervention*, vol. 14, 2011, pp. 623–630.
- [35] M. von Siebenthal, G. Székely, A. Lomax, P. Cattin, Inter-subject modelling of liver deformation during radiation therapy, in: *Medical Image Computing and Computer-Assisted Intervention: MICCAI ... International Conference on Medical Image Computing and Computer-Assisted Intervention*, vol. 10, 2007, pp. 659–666.
- [36] L. Bouarfa, P.P. Jonker, J. Dankelman, Discovery of high-level tasks in the operating room, *J. Biomed. Inform.* 44 (2011) 455–462.
- [37] L. Bouarfa, J. Dankelman, Workflow mining and outlier detection from clinical activity logs, *J. Biomed. Inform.* 45 (2012) 1185–1190.
- [38] S. Franke, T. Neumuth, A framework for event-driven surgical workflow assistance, *Biomed. Tech.* 59 (2014) S431–S434.